



CHORUS

This is the accepted manuscript made available via CHORUS. The article has been published as:

Error-Transparent Quantum Gates for Small Logical Qubit Architectures

Eliot Kapit

Phys. Rev. Lett. **120**, 050503 — Published 1 February 2018

DOI: [10.1103/PhysRevLett.120.050503](https://doi.org/10.1103/PhysRevLett.120.050503)

Error-transparent quantum gates for small logical qubit architectures

Eliot Kapit

Department of Physics and Engineering Physics, Tulane University, New Orleans, LA 70118

One of the largest obstacles to building a quantum computer is gate error, where the physical evolution of the state of a qubit or group of qubits during a gate operation does not match the intended unitary transformation. Gate error stems from a combination of control errors and random single qubit errors from interaction with the environment. While great strides have been made in mitigating control errors, intrinsic qubit error remains a serious problem that limits gate fidelity in modern qubit architectures. Simultaneously, recent developments of small error-corrected logical qubit devices promise significant increases in logical state lifetime, but translating those improvements into increases in gate fidelity is a complex challenge. In this Letter, we construct protocols for gates on and between small logical qubit devices which inherit the parent device’s tolerance to single qubit errors which occur at any time before or during the gate. We consider two such devices, a passive implementation of the three-qubit bit flip code, and the author’s own Very Small Logical Qubit design, and propose error-tolerant gate sets for both. The effective logical gate error rate in these models displays superlinear error reduction with linear increases in single qubit lifetime, proving that passive error correction is capable of increasing gate fidelity. Using a standard phenomenological noise model for superconducting qubits, we demonstrate a realistic, universal one- and two-qubit gate set for the VSLQ, with error rates an order of magnitude lower than those for same-duration operations on single qubits or pairs of qubits. These developments further suggest that incorporating small logical qubits into a measurement based code could substantially improve code performance.

To build a fault-tolerant, error-corrected quantum computer, every code operation (one- and two-qubit gates, state preparation, measurement and idling) must be performed to extremely high fidelity [1, 2]. While such fidelities have been achieved in single qubit gates [3–7], improving two-qubit gate performance is considerably more difficult [8–11]. Experimentally realized gate error is not far below threshold rate, primarily limited by random single qubit error mid-gate. Further, the classical processing required for a code involving millions of physical qubits is daunting. Increasing the cycle time to reduce this burden increases error rates, further degrading code performance. An improved qubit primitive with much higher idle coherence and two-qubit gate fidelity could thus make it easier to implement a topological code.

Toward this end, small logical qubit designs, where a quantum degree of freedom is encoded across multiple physical devices and protected by autonomous error correction, have attracted much recent interest [12–20], including the first experimental demonstration of QEC exceeding breakeven [21]. However, due to these systems’ more complex Hilbert spaces, increased idle lifetime does not usually imply improved gate fidelity. To achieve this, we extend the “error-transparent” quantum gates of Vy *et al* [22] to autonomous logical qubits [44]. In these protocols, the gate Hamiltonian is tuned to commute with single-qubit errors, when acting on the logical state manifold, *at all times during the gate operation*. Specifically, if our logical qubit has logical states $|\psi_{Li}\rangle$, suffers random errors $\{E_j\}$, and is operated by time-dependent gate Hamiltonians $\{H_{Gk}\}$, error transparency is achieved if:

$$[E_j, H_{Gk}] |\psi_{Li}\rangle = 0 \quad \forall \{i, j, k\}. \quad (1)$$

The presence of the logical states in this definition is critical, as the operators arising from the commutators $[E_j, H_{Gk}]$ cannot in general be set to zero, though they *can* be chosen to annihilate the $|\psi_{Li}\rangle$. This criteria ensures that subsequent error correction will recover the transformed logical state regardless of when the error occurred. The error rate of such a gate in the ideal limit would thus decrease as $T_g T_R / T_1^2$ (where T_g, T_R and T_1 are the gate, error correction and random error timescales, respectively), leading to large fidelity improvements.

These gates can be thought of as extending the concept of a decoherence-free-subspace [23–25] for small logical qubits, to mitigate errors against which a DFS cannot be directly formulated. They complement recent work for cat codes [15, 26, 27], though those schemes fall short of a complete, universal error-transparent gate set (ETGS). We will outline the principles of an ETGS in a passive implementation of the three-qubit bit flip code [12–14, 19], describe a realistic ETGS for the author’s VSLQ architecture [18], and benchmark both through numerical simulation. We will demonstrate super-linear decreases in gate error with increased T_1 , and show that two-qubit gate error rates in the low 10^{-4} range are achievable at current base qubit coherence.

Error transparent gates for a passive bit flip code: To demonstrate the principles of error transparency, we first consider a passive implementation of the three-qubit bit flip code (PBFC). This small logical qubit has Hamiltonian $H_P = -J(\sigma_1^z \sigma_2^z + \sigma_2^z \sigma_3^z + \sigma_1^z \sigma_3^z)$, and allows for random σ^x errors to be passively corrected through resonant energy transfer to a lossy subsystem. Independent of the details of the device’s implementation, we consider a white noise error model of random σ^x

spin flips at a rate Γ_P combined with incoherent “repair” operations R_i at a rate Γ_R . The density matrix ρ of a PBFC evolves under the Lindblad equation [28]

$$\begin{aligned} \partial_t \rho &= \sum_{i=1}^3 \Gamma_P (\sigma_i^x \rho \sigma_i^x - \rho) + \left(R_i \rho R_i^\dagger - \frac{1}{2} \{ \rho, R_i^\dagger R_i \} \right) \\ R_i &\equiv \frac{\sqrt{\Gamma_R}}{4} \sigma_i^x \left((1 - \sigma_i^z \sigma_{i-1}^z) (1 - \sigma_i^z \sigma_{i+1}^z) \right). \end{aligned} \quad (2)$$

The logical states of the PBFC are $|0_L\rangle = |000\rangle$ and $|1_L\rangle = |111\rangle$; as argued previously [12–14, 19, 20], the logical error rate for these states is given by $\Gamma_L \simeq 6\Gamma_P^2 / (3\Gamma_P + \Gamma_R)$, decreasing quadratically in Γ_P .

A good pair of logical operators for the PBFC are $Z_L \equiv \sigma_1^z$ and $X_L \equiv \sigma_1^x \sigma_2^x \sigma_3^x$. Since we only consider errors through the σ_i^x channels X_L is automatically error transparent, as it commutes with all σ_i^x . Its fidelity is thus unaffected by single random errors. However, Z_L is not, since it anticommutes with σ_1^x . Consequently, when acting with Z_L as a gate Hamiltonian (applied for a finite time t_g), if a σ_1^x error occurs before or during the gate, the system will evolve under $-Z_L$ until the error is corrected, undoing a random fraction of the gate operation. Since the time between bit flip errors and their correction is not measurable, this is a logical error source, and the error rate of Z_L decreases only linearly with $\Gamma_P t_g$.

We now introduce an error transparent Z_L , by incorporating stabilizer terms into the gate operator itself:

$$Z_L \rightarrow \sigma_1^z (1 - (1 - \sigma_1^z \sigma_2^z) (1 - \sigma_1^z \sigma_3^z) / 2). \quad (3)$$

To see why this new Z_L commutes with all three σ_i^x , we first note that if a σ_2^x or σ_3^x error has occurred, at least one of the projectors $(1 - \sigma_1^z \sigma_2^z)$ and $(1 - \sigma_1^z \sigma_3^z)$ will still return zero (both return zero on a logical state), leaving only σ_1^z , which commutes trivially. As for σ_1^x , if we act with σ_1^x the σ_1^z eigenvalue is flipped and σ_1^z returns the opposite eigenvalue of the parent logical state, so that $Z_L \rightarrow -Z_L$. If this occurs in the middle of the gate pulse, this will partially invert the full Z_L operation and cause a logical error. However, σ_1^x also breaks two $\sigma_i^z \sigma_j^z$ bonds, which causes the product of projectors in (3) to return -2 , flipping the sign again and allowing the gate to evolve as intended. Of course, two simultaneous σ^x errors will still cause a logical error. A gate set which is capable of applying X_L and Z_L partially and in combination is capable of implementing arbitrary single-PBFC rotations. Performance of the error-transparent Z_L is benchmarked in FIG. 1. Gate fidelity for both the PBFC and VSLQ below was found by evolving the system’s Lindblad equation until the decay rate equilibrates (eliminating spurious short-time behavior; this occurs when $t \simeq 1/\Gamma_R$), simulating the gate operation with noise, and averaging the resulting error rate $1 - \text{Tr}(\rho \cdot \rho_{ideal})$ (where ρ is the evolved density matrix and ρ_{ideal} models error-free evolution under the same gate) over all six combinations of initial X, Y, Z eigenstates (thirty-six for two-qubit gates).

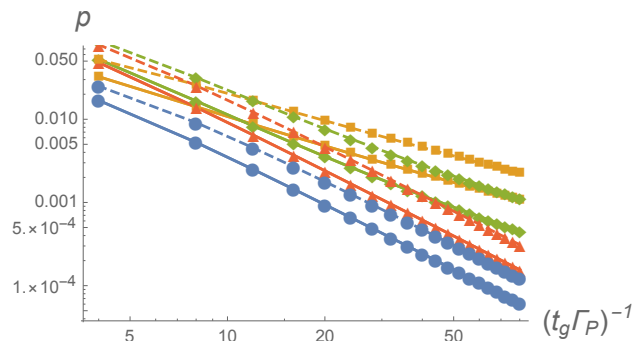


FIG. 1: (Color online) Error rate for gate operations in the passive bit flip code described in the text and Eq. 2. Solid lines correspond to a passive “repair” rate $\Gamma_R = 10/t_g$, and dashed lines correspond to $\Gamma_R = 5/t_g$, where t_g is the gate duration. The processes plotted are idling (blue, circles), the bare single-device Z_L operation ($H_G = \sigma_1^z$; gold, squares), bare CZ between two devices (green, diamonds), and the error-transparent CZ with an entangling gate Hamiltonian given by Eq. 4 (red, triangles). Error rates for error transparent Z_L are nearly identical to idling. As the error-transparent gate Hamiltonians commute with single qubit errors their error rate decreases nearly quadratically in decreasing Γ_P . In contrast, the bare operations do not commute with local σ_i^x errors, and exhibit scaling which is little better than linear. These results demonstrate that error transparent gate protocols meeting the criteria (1) can improve gate fidelity through passive, autonomous error correction.

Building on these results, we can also construct a two-PBFC entangling gate. At the operator level, on qubits A and B control-Z can be expressed as $CZ = \exp i \frac{\pi}{4} (Z_{LA} - Z_{LB} - Z_{LA} Z_{LB})$. The single-PBFC parts of this operator can be implemented normally, though the entangling part of the operation contains a six-spin term. We can reduce this operator count to four by defining $C_{ij} \equiv (1 - \sigma_i^z \sigma_j^z) / 2$ and replacing $Z_{LA} Z_{LB}$ with

$$Z_{LA} Z_{LB} \rightarrow \sigma_{1A}^z \sigma_{1B}^z (1 - 2C_{12}^A C_{13}^A - 2C_{12}^B C_{13}^B) \quad (4)$$

The highest order term here is a four-spin term, and remarkably, CZ implemented with this operator is still error-transparent. This is because it still commutes with σ_{1A}^x and σ_{1B}^x (and trivially commutes with all other single spin errors) when acting on logical states, though it does not commute with $\sigma_{1A}^x \sigma_{1B}^x$ and can produce a logical error in that case. However, if $t_g \Gamma_P^2 / \Gamma_R \ll 1$ this is rare, and gate error still decreases quadratically in decreasing Γ_P . Performance of this gate is shown in FIG. 1.

The Very Small Logical Qubit: The PBFC has two important shortcomings: it can only correct a single error channel and error-transparent gates require continuously applying three- and four-qubit operators. To overcome these issues, we will blueprint an ETGS in the Very Small Logical Qubit architecture [18]. VSLQs protect against all common error sources to first order, and as we shall see, an error-transparent entangling gate can be imple-

mented between them using only two-qubit operations.

A VSLQ consists of a pair of transmon qubit devices, operated as three level systems, and coupled by a tunable, flux driven coupler [29] driven at high frequencies to coherently drive two- and four-photon transitions. Defining $\tilde{X}_i \equiv (|0_i\rangle\langle 2_i| + |2_i\rangle\langle 0_i|)$ and P_i^j to be the projector onto states where object i contains exactly j photons, the rotating frame VSLQ Hamiltonian, in the three level basis [45] of the left and right qubits l and r is given by:

$$H_P = -W\tilde{X}_l\tilde{X}_r + \frac{\delta}{2}(P_l^1 + P_r^1) \quad (5)$$

The ground states of the VSLQ are the two states satisfying $\tilde{X}_l\tilde{X}_r = 1$. For the simulations in this paper, we used $W = 25$ MHz and $\delta = 300$ MHz (both $\times 2\pi$). Given the phenomenological noise model for superconducting qubits of low-frequency phase noise [30–37] and white noise photon loss through the $a_{l/r}$ operators, when coupled to additional lossy elements the VSLQ acts as a logical qubit protected against all single qubit error channels. Specifically, we introduce two additional lossy “shadow” qubits or resonators [14, 38], with Hamiltonian

$$\begin{aligned} H &= H_P + H_S + H_{PS}, \quad H_S = \omega_S (a_{Sl}^\dagger a_{Sl} + a_{Sr}^\dagger a_{Sr}), \\ H_{PS} &= \Omega(t) (a_l^\dagger a_{Sl}^\dagger + a_r^\dagger a_{Sr}^\dagger + \text{H.c.}) \end{aligned} \quad (6)$$

By careful tuning of the loss rate Γ_S and coupling $\Omega(t)$ (the optimal values depend on the primary error rate Γ_P), photon losses in primary qubits convert to excitations in shadow objects, returning the VSLQ to its parent logical state. The fast decay rate of the shadow objects then eliminates these excitations, returning to the rotating frame ground state and correcting the error. While phase errors cannot be corrected in the VSLQ, the $\tilde{X}_l\tilde{X}_r$ term introduces an energy penalty which suppresses low-frequency phase noise [18, 20]. In the Supplemental Material of this paper, we quantify this suppression, provide further details about the signals used in our gate simulations, and describe realistic microwave signal combinations to implement error-transparent VSLQ operators.

Error-transparent gates for a single VSLQ: To generate an error-transparent single qubit gate set for the VSLQ, we need to construct two anticommuting “bare” X_L and Z_L operators. A natural choice is $X_L^{(\text{bare})} \equiv \tilde{X}_l$ and $Z_L^{(\text{bare})} \equiv \tilde{Z}_l\tilde{Z}_r$, where $\tilde{Z}_i \equiv P_i^2 - P_i^0$. These operators commute with H_P and anticommute with each other, and sequences of partial rotations constructed from them can implement arbitrary rotations in the logical manifold.

However, these operators are not error-transparent, since the bare operators \tilde{X}_i and \tilde{Z}_i return zero acting on a $|1\rangle$ state. If a photon loss occurs during a gate, the desired operation will not be continuously applied to the VSLQ until the photon loss is repaired, leading to a

possible logical error. To remedy this, we define:

$$\begin{aligned} X_L &\equiv \tilde{X}_l + P_l^1 \tilde{X}_r, \quad Z_L \equiv \tilde{Z}_l \tilde{Z}_r'; \\ &\left(\tilde{Z}_i' \equiv P_i^2 + P_i^1 - P_i^0 \right). \end{aligned} \quad (7)$$

Both of these operations can be implemented by adding additional signals through the VSLQ’s central SQUID; we shall now prove their error-transparency.

We first consider X_L . Consider a photon loss in the r qubit during the application of X_L as a gate Hamiltonian. Since there are by default no $|1\rangle$ states in the logical state manifold $\{|\psi_L\rangle\}$, the $P_l^1 \tilde{X}_r$ term returns zero, and $[\tilde{X}_l, a_r] = 0$ trivially, so $[a_r, X_L]|\psi_L\rangle = 0$. Similarly, if a photon is lost from the left qubit, \tilde{X}_l returns zero, but since $\tilde{X}_l\tilde{X}_r|\psi_L\rangle = 1$, $\tilde{X}_l|\psi_L\rangle = \tilde{X}_r|\psi_L\rangle$ and the system evolves identically under $P_l^1 \tilde{X}_r$, and $[a_l, X_L]|\psi_L\rangle = 0$ as well. Of course, if two or more photons are lost during the gate operation a logical error will occur, so the gate error should shrink as nearly $T_g T_R / T_{1P}^2$ as T_{1P} grows.

We now consider Z_L . Since we assume photon loss errors but no photon addition, if one of the transmons is in a $|1\rangle$ state it decayed from a $|2\rangle$ state in the logical state manifold. As \tilde{Z}' returns 1 on both $|1\rangle$ and $|2\rangle$, evolution of a logical state under the operator $\tilde{Z}_l \tilde{Z}_r'$ is unchanged by a single photon loss in either qubit. Z_L is thus similarly protected against single photon losses as X_L is. We benchmark these gates against photon loss in FIG. 2. For simplicity, our simulations restricted the VSLQ transmons to the three-level basis and assumed perfect implementation of the error-transparent operators. The only significant error source in our simulations was thus random photon loss, as control error is negligible for the long gate durations considered. Errors due to the effect of higher levels are small and can be eliminated by analytical or numerical optimization schemes [39, 40].

An error-transparent two-VSLQ gate: As in the PBFC, implementing a realistic two-VSLQ entangling gate based on the error transparent operators (7) is a subtle challenge. Since X_L and Z_L are constructed from two-qubit operations, products of them acting on two VSLQ copies involve complicated three- and four-qubit operations. One could engineer these operations using gadgets as in [41], at the cost of increased complexity and additional error channels; we avoid this route here.

To generate an error-transparent CZ gate, we imagine a pair of VSLQs A and B , coupled by flux tunable couplers [9, 42], which are driven off-resonantly to induce potential terms between qubits in A and B . If both VSLQ copies are in the logical state manifold, the entangling $Z_{LA}Z_{LB}$ operation can be generated perturbatively:

$$\begin{aligned} H_{CZ}(t) &= g(t) (\tilde{Z}_{lA} \tilde{Z}_{lB} + \tilde{Z}_{rA} \tilde{Z}_{rB}); \\ &\rightarrow -\frac{g(t)^2}{2W} \tilde{Z}_{lA} \tilde{Z}_{lB} \tilde{Z}_{rA} \tilde{Z}_{rB} + O(g(t)^4). \end{aligned} \quad (8)$$

Here, $g(t) \ll W$. The second line arises at second order in perturbation theory, with a factor of 2 from combinatorics canceled by the energy cost $4W$ of transiently flipping both VSLQ copies into $\tilde{X}_l \tilde{X}_r = -1$ states from a $\tilde{Z}_{lA} \tilde{Z}_{lB}$ or $\tilde{Z}_{rA} \tilde{Z}_{rB}$ term. However, it is only correct when both VSLQs are in logical states! If a single photon is lost in one of the VSLQ copies, the action of a $\tilde{Z}_A \tilde{Z}_B$ term now only has an energy cost of $2W$, as the $\tilde{X}_l \tilde{X}_r$ term in H_P (5) returns zero on $|1\rangle$ states and thus commutes with single \tilde{Z} terms. This suggests that we can achieve error transparency by defining $\tilde{Z}_i'' \equiv P_i^2 + \frac{1}{2}P_i^1 - P_i^0$ and engineering the Hamiltonian

$$\begin{aligned} H_{CZ}(t) &\rightarrow g(t) \left(\tilde{Z}_{lA}'' \tilde{Z}_{lB}'' + \tilde{Z}_{rA}'' \tilde{Z}_{rB}'' \right) \\ &\rightarrow -\frac{g(t)^2}{2W} \tilde{Z}'_{lA} \tilde{Z}'_{lB} \tilde{Z}'_{rA} \tilde{Z}'_{rB} + O(g(t)^4). \end{aligned} \quad (9)$$

This new H_{CZ} will have the same perturbative coefficient (to $O(g^2)$) and evolve identically even if a single photon is lost. The bare \tilde{Z}'' matrix element is cut in half when acting on a $|1\rangle$ state, but a $|1\rangle$ state only arises from $|2\rangle$ state decay (hence the replacement of \tilde{Z}'' with \tilde{Z}'); this balances the reduced energy denominator of $2W$. The expression (9) is only correct if one or zero photons have been lost (from any of the four transmons); two losses produce an error, but at high T_{1P} this is rare, decreasing gate error nearly quadratically in increasing T_{1P} .

We can benchmark the performance of these gates numerically. Using relatively un-optimized Gaussian or Tanh waveforms, we demonstrate super-linear scaling of gate error, with the error rate for a CZ of 200 or 400 ns total gate time best fit by $p(T_{1P}) = 0.0057/T_{1P} + 0.253/T_{1P}^2$ ($p = 1.48 \times 10^{-4}$ at $T_{1P} = 64\mu\text{s}$) and $0.0064/T_{1P} + 0.380/T_{1P}^2$, respectively. The quadratic term thus dominates until T_{1P} is large; gate error in absence of random error processes is $\sim 10^{-7}$.

State measurement and conclusions: Adopting the protocol of Didier *et al* [43], we can achieve error-transparent, non-destructive state measurement for superconducting small logical qubits. Specifically, if we couple an error-transparent gate operator G_i to the displacement of a readout resonator $G_i(a_R^\dagger + a_R)$, the resonator state will track the eigenvalue of G_i to measure it directly. Alternatively, one can make multiple simultaneous measurements and majority vote; for the PBFC measuring all three σ_i^z tolerates a single σ_i^x error, and for the VSLQ directly measuring both \tilde{X}_l and \tilde{X}_r tolerates a single photon loss, since one of the \tilde{X} operators will return zero but the other will still return the correct value. Assuming perfect operator implementation, we thus expect measurement error $p \propto T_M T_R / T_{1P}^2$, where T_M is the measurement time, an identical quadratic improvement.

We have presented a scheme for mid-gate passive error correction in small logical qubits, allowing gate operations to inherit the parent devices' tolerance to single-

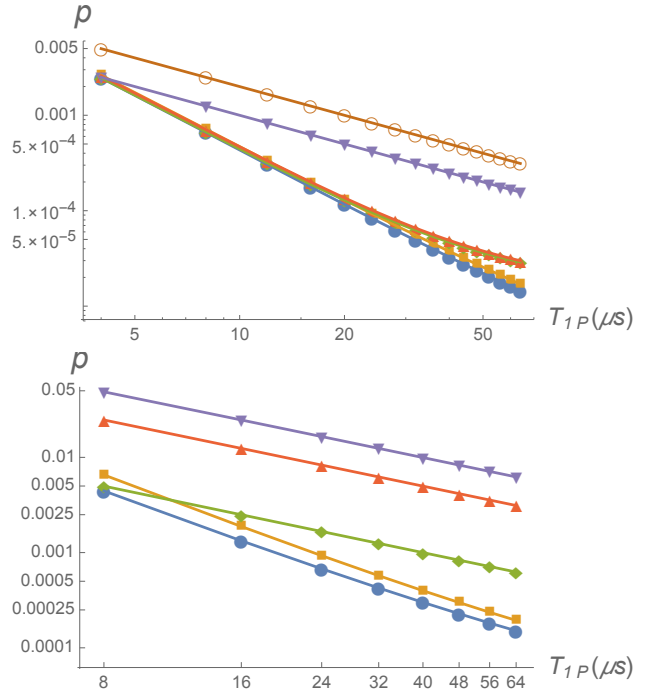


FIG. 2: (Color online) Gate fidelities for the VSLQ. Top: Simulated fidelity for single-VSLQ error-transparent gate operations using the error-transparent operators (7), averaged over the logical Bloch sphere, with pulsed error correction drives and gate duration of $t_g = 200$ ns. Here, we plot error rates for idling (blue, circles), logical X (gold, squares), Z (green, diamonds) and Hadamard (brown, squares; nearly identical to Z_L error rate). For comparison, we include default error rates $1 - e^{-T_g/2T_{1P}}$ for gate durations of 20 (purple, triangles) and 40 (brown, open circles) ns, assuming no control error. Bottom: fidelity of two-qubit gates, for photon loss rate T_{1P} between 8 and 64 μs . Here we plot the average error rate p for error transparent CZ using gate Hamiltonian (9), with durations of 200 ns (blue, circles) and 400 ns (gold, squares). For comparison, we plot bare two-qubit CZ gate error from photon losses for a pair of single transmons $1 - e^{-T_g/T_{1P}}$ for $T_g = 40$ ns (green, diamonds), 200 ns (red, triangles), and 400 ns (purple, triangles), with dephasing and control errors absent.

qubit errors. The simulated performance of these gates is extremely promising, with two-qubit gate error rates in the low 10^{-4} range achievable for experimentally accessible T_1 . Combined with robust measurement protocols, we have outlined the essential ingredients required for a “dissipative subsystem code,” where small logical qubit copies replace single qubits in a topological code, improving the operation fidelity by an order of magnitude. However, it is important to caution that leakage (e.g. short-lived populations of $|1_l 1_r\rangle$ or $\tilde{X}_l \tilde{X}_r = -1$ states in the VSLQ) must be rigorously analyzed before making quantitative predictions about code performance.

ACKNOWLEDGEMENTS

We would like to thank Jonathan DuBois, Eric Holland, Yao Lu, David Rodriguez-Perez, Yaniv Rosen and David Schuster for useful discussions. This work was supported by Lawrence Livermore National Laboratory under LLNL-LDRD (16-SI-004), by the Louisiana Board of Regents RCS grant LEQSF(2016-19)-RD-A-19, and by the National Science Foundation grant PHY-1653820.

-
- [1] A. G. Fowler, M. Mariantoni, J. M. Martinis, and A. N. Cleland, *Phys. Rev. A* **86**, 032324 (2012).
- [2] B. M. Terhal, *Rev. Mod. Phys.* **87**, 307 (2015).
- [3] J. M. Chow, J. M. Gambetta, A. D. Corcoles, S. T. Merkel, J. A. Smolin, C. Rigetti, S. Poletto, G. A. Keefe, M. B. Rothwell, J. R. Rozen, et al., *Phys. Rev. Lett.* **109**, 060501 (2012).
- [4] R. Barends, J. Kelly, A. Megrant, A. Veitia, D. Sank, E. Jeffrey, T. C. White, J. Mutus, A. G. Fowler, B. Campbell, et al., *Nature* **508**, 500 (2014).
- [5] A. D. Corcoles, E. Magesan, S. J. Srinivasan, A. W. Cross, M. Steffen, J. M. Gambetta, and J. M. Chow, *Nature communications* **6** (2015).
- [6] D. C. McKay, C. J. Wood, S. Sheldon, J. M. Chow, and J. M. Gambetta, *Physical Review A* **96**, 022330 (2017).
- [7] M. Rol, C. Bultink, T. O'Brien, S. de Jong, L. Theis, X. Fu, F. Luthi, R. Vermeulen, J. de Sterke, A. Bruno, et al., *Physical Review Applied* **7**, 041001 (2017).
- [8] J. Kelly, R. Barends, B. Campbell, Y. Chen, Z. Chen, B. Chiaro, A. Dunsworth, A. G. Fowler, I.-C. Hoi, E. Jeffrey, et al., *Phys. Rev. Lett.* **112**, 240504 (2014), URL <http://link.aps.org/doi/10.1103/PhysRevLett.112.240504>.
- [9] D. C. McKay, S. Filipp, A. Mezzacapo, E. Magesan, J. M. Chow, and J. M. Gambetta, arXiv:1604.03076 (2016).
- [10] H. Paik, A. Mezzacapo, M. Sandberg, D. T. McClure, B. Abdo, A. D. Corcoles, O. Dial, D. F. Bogorin, B. L. T. Plourde, M. Steffen, et al., arXiv:1606.00685 (2016).
- [11] J. Z. Blumoff, K. Chou, C. Shen, M. Reagor, C. Axline, R. T. Brierley, M. P. Silveri, C. Wang, B. Vlastakis, S. E. Nigg, et al., *Phys. Rev. X* **6**, 031041 (2016), URL <http://link.aps.org/doi/10.1103/PhysRevX.6.031041>.
- [12] J. Kerckhoff, H. I. Nurdin, D. S. Pavlichin, and H. Mabuchi, *Phys. Rev. Lett.* **105**, 040502 (2010), URL <http://link.aps.org/doi/10.1103/PhysRevLett.105.040502>.
- [13] J. Cohen and M. Mirrahimi, *Phys. Rev. A* **90**, 062344 (2014).
- [14] E. Kapit, M. Hafezi, and S. H. Simon, *Physical Review X* **4**, 031039 (2014).
- [15] M. Mirrahimi, Z. Leghtas, V. V. Albert, S. Touzard, R. J. Schoelkopf, L. Jiang, and M. H. Devoret, *New J. Phys.* **16**, 045014 (2014).
- [16] L. Sun, A. Petrenko, Z. Leghtas, B. Vlastakis, G. Kirchmair, K. M. Sliwa, A. Narla, M. Hatridge, S. Shankar, J. Blumoff, et al., *Nature* **511**, 444 (2014).
- [17] Z. Leghtas, S. Touzard, I. M. Pop, A. Kou, B. Vlastakis, A. Petrenko, K. M. Sliwa, A. Narla, S. Shankar, M. J. Hatridge, et al., *Science* **347**, 6224 (2015).
- [18] E. Kapit, *Phys. Rev. Lett.* **116**, 150501 (2016).
- [19] F. Reiter, A. Sørensen, P. Zoller, and C. Muschik, arXiv preprint arXiv:1702.08673 (2017).
- [20] E. Kapit, *Quantum Science and Technology* **2**, 033002 (2017).
- [21] N. Ofek, A. Petrenko, R. Heeres, P. Reinhold, Z. Leghtas, B. Vlastakis, Y. Liu, L. Frunzio, S. M. Girvin, L. Jiang, et al., *Nature* **536**, 441 (2016).
- [22] O. Vy, X. Wang, and K. Jacobs, *New Journal of Physics* **15**, 053002 (2013).
- [23] D. A. Lidar, I. L. Chuang, and K. B. Whaley, *Physical Review Letters* **81**, 2594 (1998).
- [24] A. Beige, D. Braun, B. Tregenna, and P. L. Knight, *Physical Review Letters* **85**, 1762 (2000).
- [25] D. A. Lidar, *Quantum Information and Computation for Chemistry: Advances in Chemical Physics Volume 154* pp. 295–354 (2014).
- [26] V. V. Albert, C. Shu, S. Krastanov, C. Shen, R.-B. Liu, Z.-B. Yang, R. J. Schoelkopf, M. Mirrahimi, M. H. Devoret, and L. Jiang, *Phys. Rev. Lett.* **116**, 140502 (2016).
- [27] J. Cohen, W. C. Smith, M. H. Devoret, and M. Mirrahimi, arXiv:1611.01219 (2016).
- [28] C. Gardiner and P. Zoller, *Quantum Noise: A Handbook of Markovian and Non-Markovian Quantum Stochastic Methods with Applications to Quantum Optics* (Springer, 2004).
- [29] E. Kapit, *Phys. Rev. A* **92**, 012302 (2015).
- [30] J. Martinis, S. Nam, J. Aumentado, K. M. Lang, and C. Urbina, *Phys. Rev. B* **67**, 094510 (2003).
- [31] G. Ithier, E. Collin, P. Joyez, P. J. Meeson, D. Vion, D. Esteve, F. Chiarello, A. Shnirman, Y. Makhlin, J. Schrieffer, et al., *Phys. Rev. B* **72**, 134519 (2005).
- [32] F. Yoshihara, K. Harrabi, A. O. Niskanen, Y. Nakamura, and J. S. Tsai, *Phys. Rev. Lett.* **97**, 167001 (2006).
- [33] J. Bylander, S. Gustavsson, F. Yan, F. Yoshihara, K. Harrabi, G. Fitch, D. G. Cory, Y. Nakamura, J.-S. Tsai, and W. D. Oliver, *Nature Physics* **7**, 565 (2011).
- [34] S. M. Anton, C. Müller, J. S. Birenbaum, S. R. O'Kelley, A. D. Fefferman, D. S. Golubev, G. C. Hilton, H.-M. Cho, K. D. Irwin, F. C. Wellstood, et al., *Phys. Rev. B* **85**, 224505 (2012).
- [35] F. Yan, S. Gustavsson, J. Bylander, X. Jin, F. Yoshihara, D. G. Cory, Y. Nakamura, T. P. Orlando, and W. D. Oliver, *Nature Communications* **4**, 2337 (2013).
- [36] E. Paladino, Y. M. Galperin, G. Falci, and B. L. Altshuler, *Rev. Mod. Phys.* **86**, 361 (2014).
- [37] P. J. J. O'Malley, J. Kelly, R. Barends, B. Campbell, Y. Chen, Z. Chen, B. Chiaro, A. Dunsworth, A. G. Fowler, I.-C. Hoi, et al., *Phys. Rev. Applied* **3**, 044009 (2015).
- [38] Y. Lu, S. Chakram, N. Leung, N. Earnest, R. K. Naik, Z. Huang, P. Groszkowski, E. Kapit, J. Koch, and D. I. Schuster, *Phys. Rev. Lett.* **119**, 150502 (2017), URL <https://link.aps.org/doi/10.1103/PhysRevLett.119.150502>.
- [39] N. Khaneja, T. Reiss, C. Kehlet, T. Schulte-Herbrüggen, and S. J. Glaser, *J. Mag. Res.* **172**, 296 (2005).
- [40] F. Motzoi, J. M. Gambetta, P. Rebentrost, and F. K. Wilhelm, *Phys. Rev. Lett.* **103**, 110501 (2009).
- [41] E. Kapit, J. T. Chalker, and S. H. Simon, *Phys. Rev. A* **91**, 062324 (2015).
- [42] Y. Chen, C. Neill, P. Roushan, N. Leung, M. Fang, R. Barends, J. Kelly, B. Campbell, Z. Chen, B. Chiaro, et al., *Phys. Rev. Lett.* **113**, 220502 (2014), URL <http://>

link.aps.org/doi/10.1103/PhysRevLett.113.220502.

- [43] N. Didier, J. Bourassa, and A. Blais, *Phys. Rev. Lett.* **115**, 203601 (2015).
- [44] Note that error transparency is distinct from the more general notion of fault tolerance, as fault tolerance is typically interpreted as the ability to exponentially reduce logical error rates from a polynomial increase in circuit complexity. The small logical qubit circuits considered here do not have an obvious scaling path, but perform extremely well against single error events, and could po-

tentially improve code performance by replacing single qubits in a larger measurement-based code.

- [45] The continuously increasing nonlinearity allows us to effectively ignore the $|3\rangle$ and $|4\rangle$ states of each transmon. Mixing with these states will create small higher order corrections, which can be easily compensated by additional signals to counter their effects. For clarity and simplicity we will ignore these effects here.